APPLIED AND ENVIRONMENTAL MICROBIOLOGY, Apr. 1992, p. 1164–1174 Vol. 58, No. 4
0099-2240/92/041164-11$02.00/0

Microsensor Measurements of Sulfate Reduction and Sulfide Oxidation in Compact Microbial Communities of Aerobic Biofilms

MICHAEL KÜHL* AND BO BARKER JØRGENSEN

Department of Ecology and Genetics, University of Aarhus, Ny Munkegade, DK-8000 Aarhus C, Denmark

Received 8 November 1991/Accepted 10 January 1992

The microzonation of O_2 respiration, H_2S oxidation, and SO_4^{2-} reduction in aerobic trickling-filter biofilms was studied by measuring concentration profiles at high spatial resolution (25 to 100 μm) with microsensors for O_2, S^{2-}, and pH. Specific reaction rates were calculated from measured concentration profiles by using a simple one-dimensional diffusion reaction model. The importance of electron acceptor and electron donor availability for the microzonation of respiratory processes and their reaction rates was investigated. Oxygen respiration was found in the upper 0.2 to 0.4 mm of the biofilm, whereas sulfate reduction occurred in deeper, anoxic parts of the biofilm. Sulfate reduction accounted for up to 50% of the total mineralization of organic carbon in the biofilms. All H_2S produced from sulfate reduction was reoxidized by O_2 in a narrow reaction zone, and no H_2S escaped to the overlying water. Turnover times of H_2S and O_2 in the reaction zone were only a few seconds owing to rapid bacterial H_2S oxidation. Anaerobic H_2S oxidation with NO_3^- could be induced by addition of nitrate to the medium. Total sulfate reduction rates increased when the availability of SO_4^{2-} or organic substrate increased as a result of deepening of the sulfate reduction zone or an increase in the sulfate reduction intensity, respectively.

Biofilms and microbial mats are compact microbial communities that exhibit high specific rates of metabolic processes (28, 29). The high activity in these systems is due to both dense populations of microorganisms and a high availability of organic substrates. Large populations of phototrophic algae and bacteria in microbial mats and photosynthetic biofilms can act as sources of organic substrate as a result of excretion of photosynthate in the light (83). Heterotrophic biofilms found in sewers or wastewater treatment plants receive most of their substrates from water loaded with nutrients and organic matter (51).

Despite a typical thickness of only a few millimeters, a vertical zonation of respiratory processes similar to the zonations in aquatic sediments can be found in biofilms and microbial mats (6, 68). The use of microelectrodes has made it possible to study such microzonations at a spatial resolution of less than 100 μm (72). Oxygen respiration and photosynthesis in biofilms (8, 12, 24, 51, 68) and microbial mats (44, 46, 70) have been investigated in detail over the last few years. Recently, the introduction of a combined oxygen/nitrous oxide microelectrode (75) and microelectrodes for ammonium and nitrate (18, 19) has made it possible also to investigate the nitrogen cycle at similar resolution (13, 62, 71, 79, 80).

Sulfide microelectrodes in combination with oxygen and pH microelectrodes have been used to investigate sulfide dynamics in microbial mats and sediments (45, 73, 82) as well as in gradient cultures of sulfur-oxidizing bacteria (16, 60, 61) but have not yet been used in biofilms. The sulfur cycle in compact microbial communities has been studied mainly by techniques with a low spatial resolution compared with the microelectrode techniques (29, 39, 77). Sulfate reduction in biofilms has therefore been quantified from mass balance calculations in anaerobic bioreactor systems (32, 33, 64) or by tracer techniques in biofilms growing on metal surfaces incubated under anaerobic conditions (55). Mass balances of sulfide fluxes across a biofilm-water interface, however, cannot describe sulfur transformations within aerobic biofilms or microbial mats because bacterial sulfide oxidation results in an internal sulfur cycle (41, 42). Combined with the high turnover rates found in biofilms and mats, this internal sulfur cycle also makes radiotracer techniques difficult to apply close to the oxic-anoxic interface, although several such studies have been done with microbial mats (2, 10, 43, 77). A technique for measuring sulfate reduction based on the insertion of a $^{35}SO_4^{2-}$-coated silver wire into microbial mats was described by Cohen (15). The spatial resolution of this technique is about 1 mm, but no data have yet been published.

We have used oxygen, pH, and sulfide microelectrodes to study the microzonation and dynamics of oxygen respiration, sulfide oxidation, and sulfate reduction at high spatial resolution in aerobic biofilms collected from a trickling filter. The goals were (i) to demonstrate the occurrence and significance of sulfate reduction in aerobic biofilms, (ii) to understand the regulation of sulfate reduction by the availability of sulfate or of organic substrate, and (iii) to analyze the coupling between sulfate reduction, sulfide oxidation, and oxygen respiration. The experiments were done under controlled laboratory conditions. Our results therefore present the principles of microbial regulation and interaction rather than in situ conditions of a trickling filter.

MATERIALS AND METHODS

Samples. Biofilms growing on illuminated stones were collected from a trickling filter at Skødstrup Sewage Treatment Plant, Skedstrup, Denmark, and transported to the laboratory. The trickling filter receives raw sewage from a

* Corresponding author.

settling tank with a sulfate concentration of 0.5 to 1 mM. All investigated biofilms were 3 to 5 mm thick and exhibited a very dense structure with a smooth surface layer of motile filamentous cyanobacteria (*Oscillatoria* sp.). Light microscopy revealed that the biofilm was composed mainly of degrading algae and cyanobacteria embedded in a matrix of bacteria and exopolymers together with large numbers of various protozoans. Throughout the biofilm large numbers of sludgeworms (*Tubifex* sp.) and dipteran larvae (*Psycoda* sp.) were found. The biofilm was carefully removed from most of the stone, leaving a small biofilm of 2 to 3 cm^2. Most of the larger worms and larvae were carefully removed from the biofilm with forceps, and the rinsed biofilms were stored in aerated tap water at 12 to 15°C for 24 to 72 h prior to measurements in the laboratory.

Microelectrodes. Concentration profiles of oxygen, pH, and sulfide in the biofilms were measured by microelectrodes manufactured in our laboratory.

(i) Oxygen microelectrode. The oxygen concentration was measured with a Clark-type oxygen microelectrode with a guard cathode (69). The electrodes had a tip diameter of 2 to 10 μm, a stirring sensitivity of <1 to 2%, and a 90% response time of <1 s. The electrodes were connected to a picoammeter and a recorder. Linear calibration of the electrodes was done in air-saturated medium above the biofilm and in the anaerobic part of the biofilm.

(ii) pH microelectrode. pH was measured with pH glass microelectrodes (72, 73) connected to a high-impedance electrometer (Keithley type 617) with a double-junction calomel electrode (Radiometer type 711) as a reference. Electrodes were calibrated at room temperature (20°C) in standard pH buffers. The pH microelectrodes had a log-linear response for H^+, and the calibration curves exhibited a slope of 52 to 60 mV/pH unit and a 90% response time of <10 to 20 s.

(iii) Sulfide microelectrode. Sulfide concentrations were measured with sulfide microelectrodes with a tip diameter of 20 to 50 μm (72, 73). The measuring circuit was the same as for pH measurements. Calibration was done in a dilution series of a sulfide standard solution buffered to the same pH as the synthetic biofilm medium (pH 7.2 to 7.3) and with the same ionic strength. The dilution was done with buffered biofilm medium carefully flushed with nitrogen to avoid oxidation of sulfide. The total sulfide concentration in the solutions was determined by the methylene blue technique (14). The total amount of dissolved H_2S, HS^-, and S^{2-} will be designated H_2S or total sulfide in the rest of the paper. Calibration curves for sulfide microelectrodes exhibited a log-linear response for 10^{-3} to 10^{-6} M H_2S with a slope of 26 to 38 mV per decade (Fig. 1). Electrode response times (90%) were dependent on the H_2S concentration and varied from <1 min for the highest total sulfide concentrations up to 10 to 15 min for the lowest. When the pH profiles showed a significant variation (>0.1 pH unit) through the biofilm, it was necessary to correct the measured sulfide profiles for the pH variation. The total sulfide concentration, S_t, in an aqueous solution can be expressed as follows (21):

$$S_t = [S^{2-}]\left(1 + \frac{a_{H^+}^2}{K_1'K_2'} + \frac{a_{H^+}}{K_2'}\right) \quad (1)$$

where K_1' and K_2' are the first and second dissociation constants, respectively, of the sulfide equilibrium system, $[S^{2-}]$ is the sulfide concentration, and a_{H^+} is the hydrogen ion activity. a_{H^+} was calculated from measured pH values. We used the following dissociation constants for sulfide, expressed as pK values: pK_1' = 7.05 (58, 59) and pK_2' = 17.1 (22, 56, 58).

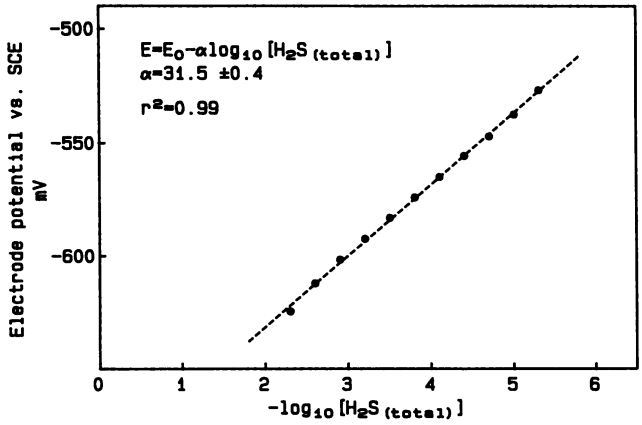

FIG. 1. Calibration of a sulfide microelectrode in a dilution series of a 1 mM Na_2S stock solution buffered with 0.1 M phosphate buffer to pH 7.2. Dilution was done with buffer solution carefully flushed with N_2. Symbols indicate measured electrode potentials in millivolts (●) as a function of pH_2S. The dashed line represents the trend curve calculated from a linear regression on the measured potentials ($r^2 > 0.99$). The slope was 31.5 mV/pH_2S.

The calibration curve for total sulfide determined at a fixed pH of 7.2 to 7.3 was transformed into a new calibration curve for $[S^{2-}]$ by using equation 1. From this curve it was possible to convert electrode readings at different pH values to actual S^{2-} concentrations. The total sulfide concentration at a position inside the biofilm could then be calculated from equation 1 by using the actual pH value measured at the same position in the biofilm.

Experimental setup. Measurements were performed at room temperature (20°C) with the biofilm submersed in a water bath containing 5 liters of medium with a known composition and pH. The synthetic medium was buffered with 0.05 to 0.1 M phosphate or Tris buffer in demineralized water and contained various amounts of sulfate, nitrate, ammonia, and organic substrate as described in the figure legends. To maintain the oxygen concentration at air saturation level, the medium was flushed continuously with air. A constant water circulation over the biofilm surface was provided by a Pasteur pipette blowing air onto the water surface. Flow velocities at 5 mm above the biofilm were determined by observing small suspended particles in the water under a dissection microscope. Flow velocities in the experiments varied from 2 to 10 cm s^{-1} and were typically around 5 cm s^{-1}. All experiments were performed in the dark to avoid photosynthesis.

Biofilm thickness. The approximate thickness of the biofilm was determined prior to microelectrode measurements by penetrating the biofilm with a thin glass capillary mounted in a micromanipulator while observing the biofilm through a dissection microscope.

Microelectrode measurements. Measurements were made with oxygen and sulfide microelectrodes mounted on the same motor-driven micromanipulator (Maertzhäuser, Germany). The tips of the oxygen and sulfide electrodes were positioned <100 μm apart in the same horizontal plane. The micromanipulator was interfaced to a desktop computer and run by a Pascal program. A pH microelectrode was mounted in a separate manually operated micromanipulator. Measurements were made in the same 1 mm^2 of a homogeneous

biofilm area by advancing the electrodes in steps of 25 to 100 μm through the biofilm. The position where the electrodes touched the biofilm surface was determined visually under a dissection microscope.

Steady state. Biofilms were incubated in the medium for at least 4 h before measurements were made; this ensured that steady-state profiles were obtained. Steady-state conditions were checked for by measuring several microprofiles within short time intervals at the same position in the biofilm.

Calculations. (i) Depth distribution of O_2 respiration, SO_4^{2-} reduction, and H_2S oxidation. Because the biofilms grow on an impermeable surface, solute exchange with the flowing-water phase occurs by diffusion across the biofilm-water interface and through the overlying diffusive boundary layer (44, 46). The shape of solute concentration profiles in the biofilm reflects the combined action of production (P), consumption (R), and diffusion as described by Fick's second law of one-dimensional diffusion (4, 67, 74):

$$\frac{\delta C(x,t)}{\delta t} = D_s \frac{\delta^2 C(x,t)}{\delta x^2} + P(x) - R(x) \quad (2)$$

where C is the solute concentration at position x and time t and D_s is the apparent diffusion coefficient of the solute in the biofilm. We used the following D_s values determined in biofilm or agar: $D_s(O_2) = 1.44 \times 10^{-5}$ cm^2 s^{-1} (23, 24) and $D_s(H_2S) = 1.39 \times 10^{-5}$ cm^2 s^{-1} (60). At steady state, equation 2 simplifies to

$$P(x) - R(x) = -D_s \frac{\delta^2 C(x)}{\delta x^2} \quad (3)$$

The specific reaction rate for the production or consumption of a solute can thus be expressed as the product of the diffusion coefficient and the curvature of the steady-state concentration profile. By assuming zero-order kinetics, it has been shown by integration of equation 3 that steady-state concentration profiles in biofilm sublayers with constant diffusion coefficients and reaction rates can be described by parabolic functions (62). Depth distributions of oxygen respiration, sulfide oxidation, and sulfate reduction were obtained by manually fitting parabolic functions to curved sections of the measured microprofiles as described by Nielsen et al. (62). The specific reaction rate in each layer was calculated from the product of the apparent diffusion coefficient and the coefficient of x^2 for the fitted parabolic function. Total reaction rates of oxygen respiration, sulfide oxidation, and sulfate reduction per unit area were then calculated by multiplying the specific rates with the thickness of the depth interval in the biofilm where the processes occurred.

(ii) Flux calculations. The one-dimensional diffusion flux of a solute, $J(x)$, is given by Fick's first law of diffusion (4):

$$J(x) = -\phi D_s \frac{\delta C(x)}{\delta x} \quad (4)$$

where ϕ is the porosity. The porosity was assumed to be close to unity and constant with depth in the biofilm. Equation 4 was used for calculations of total rates of oxygen respiration, sulfide oxidation, and sulfate reduction. Total oxygen respiration was calculated from the linear part of the O_2 profile in the diffusive boundary layer above the biofilm (46). We used a value of 2.06×10^{-5} cm^2 s^{-1} for the oxygen diffusion coefficient in water at 20°C (7). Sulfate reduction and sulfide oxidation were calculated as the flux away from the sulfate reduction zone in the biofilm. Total reaction rates based on flux calculations agreed with the rates calculated from the integrated specific reaction rates within ±10%.

RESULTS

Microzonation of O_2 respiration, H_2S oxidation, and SO_4^{2-} reduction. A typical zonation of the investigated respiratory processes is shown in Fig. 2. Oxygen penetrated only 0.4 mm into the biofilm because of high oxygen respiration (Fig. 2). Total oxygen uptake was 0.39 μmol of O_2 cm^{-2} h^{-1}. The highest specific rate of O_2 respiration was 17.5 μmol of O_2 cm^{-3} h^{-1} in the top 0.1 mm of the biofilm, where the availability of organic substrate was highest. High O_2 respiration also occurred at the narrow zone where H_2S became oxidized, 0.2 to 0.475 mm below the biofilm surface (Fig. 2B). The specific activity of H_2S oxidation was 3.5 μmol of H_2S cm^{-3} h^{-1}, giving a total H_2S oxidation of 0.095 μmol of H_2S cm^{-2} h^{-1}. The average turnover time of O_2 and H_2S in the narrow reaction zone could be calculated from the ratio of the average concentration to the average reaction rate, as shown in Table 1. Owing to the high rate of aerobic H_2S oxidation in the biofilm, the turnover times of O_2 and H_2S pools in the reaction zone were only 4.6 and 7 s, respectively.

Sulfide was produced by sulfate reduction 1.05 to 2.15 mm below the biofilm surface at a specific rate of 0.84 μmol cm^{-3} h^{-1} (Fig. 2A). Integrated sulfate reduction was found to be 0.092 μmol cm^{-2} h^{-1}. Below 2.15 mm, the constant H_2S concentration indicated that sulfide was neither produced nor consumed, as SO_4^{2-} only partly penetrated the biofilm and was depleted at the bottom of the sulfate reduction zone. Sulfide oxidation and sulfate reduction were found in two spatially separated zones. The linear H_2S profile between the two zones indicated that there was no net production or consumption of H_2S diffusing upwards to the H_2S oxidation zone. No indications of sulfide oxidation with nitrate were found, although NO_3^- was present in the medium.

Sulfate reduction as a function of sulfate concentration. The total rate of SO_4^{2-} reduction increased with increasing SO_4^{2-} concentration in the medium. In a 4.5-mm-thick biofilm incubated in the same medium with 0.5 mM (Fig. 2A), 1 mM (Fig. 3A), and 1.5 mM (Fig. 3B) SO_4^{2-}, the respective total rates were 0.092, 0.114, and 0.120 μmol cm^{-2} h^{-1}. Although the total activity increased, the specific SO_4^{2-} reduction rate was found to decrease with increasing SO_4^{2-} levels in the medium. Maximum specific rates were 0.84, 0.65, and 0.47 μmol cm^{-3} h^{-1} for 0.5, 1, and 1.5 mM SO_4^{2-}, respectively. The observed increase in the total SO_4^{2-} reduction was due to a deeper sulfate reduction zone at higher SO_4^{2-} levels in the medium. With 0.5 mM SO_4^{2-} in the medium, SO_4^{2-} was limiting for sulfate reduction below 2.1 mm (Fig. 2A), whereas SO_4^{2-} penetrated down to 4 mm with 1.5 mM SO_4^{2-} in the medium (Fig. 3B).

Sulfate reduction as a function of the organic substrate. The availability of the organic substrate for biofilm metabolism had a pronounced effect on oxygen respiration and sulfate reduction. In a 3.5-mm-thick biofilm incubated with 0.8 mM SO_4^{2-} and no added organic substrate, the total respiration rates were 0.42 μmol of O_2 cm^{-2} h^{-1} and 0.084 μmol of SO_4^{2-} cm^{-2} h^{-1}. The specific SO_4^{2-} reduction activity of 0.31 to 0.33 μmol cm^{-3} h^{-1} was evenly distributed throughout the biofilm below 0.7 mm, and the pH was almost constant at 7.3 (Fig. 4A). The same biofilm incubated with 0.8 mM SO_4^{2-} and 5 mM glucose exhibited increased rates of O_2 respiration (0.53 μmol cm^{-2} h^{-1}) and SO_4^{2-} reduction (0.21 μmol cm^{-2} h^{-1}). An increase in the overall respiratory

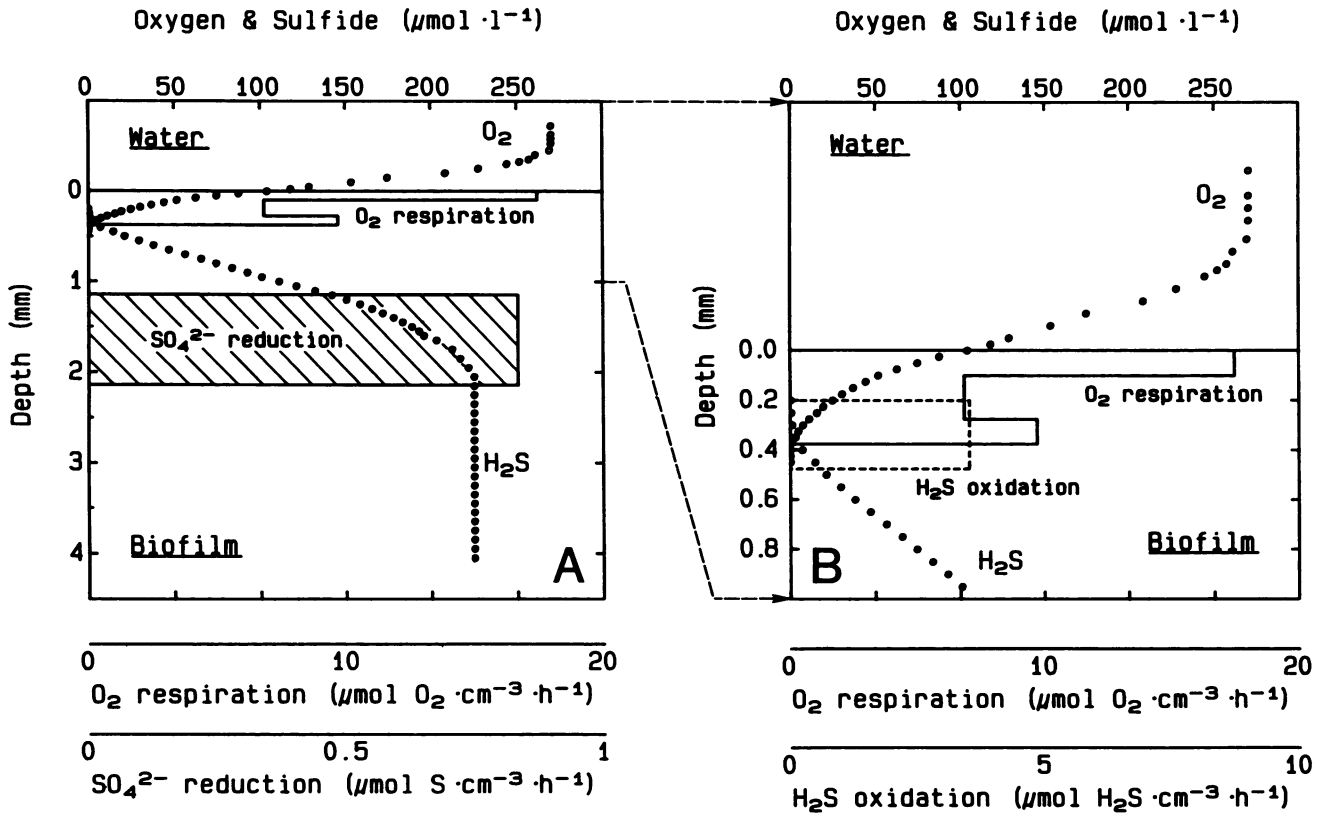

FIG. 2. Steady-state concentration profiles of O_2 (○) and H_2S (●) measured in a 4.5-mm-thick biofilm incubated in 50 mM phosphate-buffered medium (pH 7.2) containing 0.5 mM each of glucose, NO_3^-, NH_4^+, and SO_4^{2-}. The pH varied by <0.1 pH unit in the uppermost 4 mm (data not shown). The microzonation and specific reaction rates of O_2 respiration and SO_4^{2-} reduction (A) and H_2S oxidation (B) were modeled from the measured profiles and are indicated by boxes. Note the expanded depth scale in panel B.

activity was also reflected by a sharp decrease in the pH from 7.3 to 6.3 through the oxic zone, with a minimum just below the H_2S oxidation zone (Fig. 4B). Below 0.5 mm the pH was almost constant around pH 6.3. The increase in total SO_4^{2-} reduction (Fig. 4B) was due to an increased specific activity in the upper 0.7 to 1.75 mm relative to the control without organic substrate. The specific activity in this zone increased fivefold from 0.31 to 1.56 μmol cm^{-3} h^{-1}.

Induction of anaerobic sulfide oxidation by nitrate. It was possible to induce anaerobic sulfide oxidation by adding nitrate to the biofilm medium. A 3.5-mm-thick biofilm was first incubated with 0.8 mM SO_4^{2-} in the medium (Fig. 5A and B). Total rates of respiration were 0.70 μmol of O_2 cm^{-2} h^{-1} and 0.14 μmol of SO_4^{2-} cm^{-2} h^{-1}. Sulfate reduction was evenly distributed in the biofilm below 0.6 mm. Sulfide oxidation was closely associated with the O_2 respiration zone and occurred over a depth interval of 0.2 mm with a specific activity of 6.9 μmol cm^{-3} h^{-1} (Fig. 5B). After addition of 0.5 mM NO_3^- to the medium, profiles of O_2 concentration, pH, and H_2S concentration were measured at short time intervals (data not shown). The time series showed a gradual separation of the O_2 and H_2S profiles until 16 h after addition of NO_3^-, when the last set of profiles were measured (Fig. 5C). H_2S was depleted 0.5 mm below the biofilm surface, whereas O_2 penetration was only 0.25 mm, showing the presence of an anaerobic H_2S oxidation zone (Fig. 5D). Anaerobic H_2S oxidation occurred over a 0.5-mm-thick zone with a specific activity of 1.75 μmol cm^{-3} h^{-1}. O_2 respiration was unaffected by the presence of NO_3^-, because the same O_2 penetration depth (0.25 mm) and specific activity (25 to 29 μmol cm^{-3} h^{-1}) were observed before and after addition of NO_3^-, giving a total rate of 0.67 μmol of O_2 cm^{-2} h^{-1}. Sulfate reduction activity started immediately below the anaerobic H_2S oxidation zone. Total sulfate reduction decreased to 0.089 μmol cm^{-2} h^{-1} as a result of both a lower specific activity and a compressed sulfate reduction zone (Fig. 5C). The specific sulfate reduction activity decreased from 0.50 to 0.38 μmol of SO_4^{2-} cm^{-3} h^{-1} during the experiment. A possible explanation could be an overall depletion of available electron donors for sulfate-reduction during the 16-h experiment or an increased competition for electron donors with denitrifying bacteria when denitrification was stimulated by the addition of nitrate.

TABLE 1. Reaction rate and turnover time for O_2 and H_2S in the H_2S-oxidizing zone[a]

Substrate	Reaction zone (μm)	Avg concn (μmol/liter)	Reaction rate (μmol/cm^3/h)	Consumption (μmol/cm^2/h)	Turnover time (s)
O_2	175	10.5	8.2[b]	0.144[c]	4.6
H_2S	275	6.7	3.5	0.095	7.0

[a] Calculations were done with data presented in Fig. 2.
[b] Average rate of O_2 respiration in the H_2S oxidation zone.
[c] Reaction rate multiplied with depth of reaction zone. The H_2S/O_2 consumption ratio was 0.66.

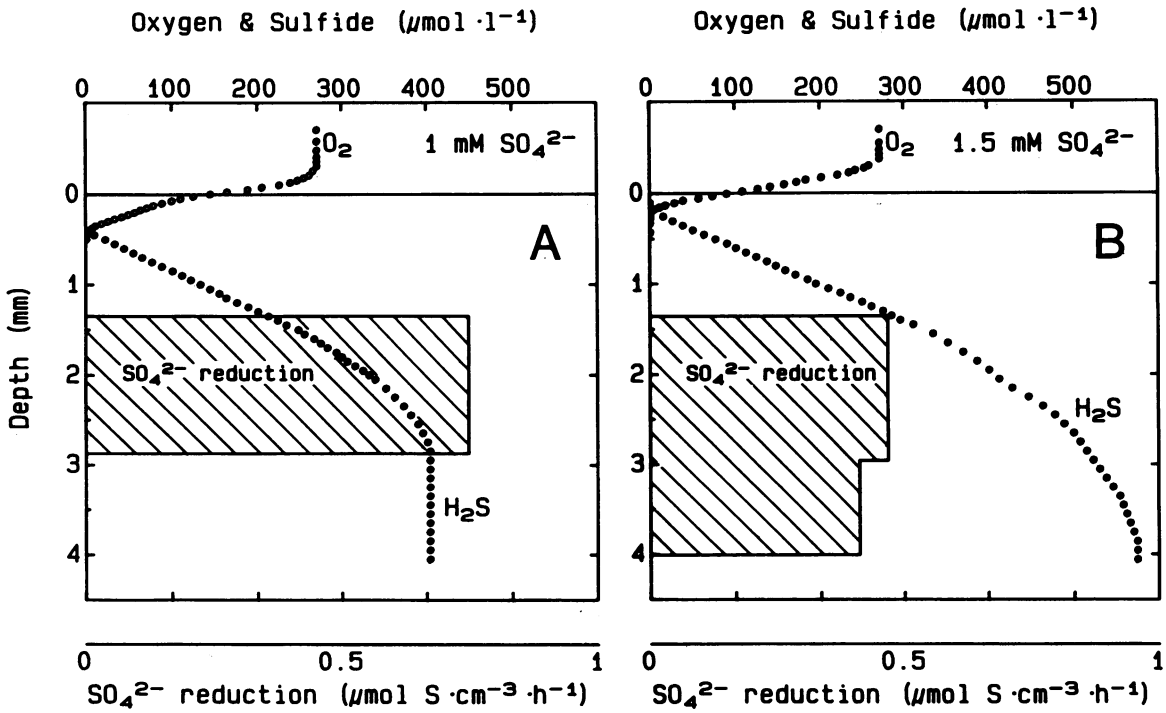

FIG. 3. Sulfate reduction as a function of sulfate concentration in the overlying water. The 4.5-mm-thick biofilm was incubated in 50 mM phosphate-buffered medium (pH 7.2) containing 0.5 mM each of glucose, NO_3^-, and NH_4^+, with 1 mM SO_4^{2-} (A) or 1.5 mM SO_4^{2-} (B). The pH varied by <0.1 pH unit in the uppermost 4 mm of the biofilm (data not shown). Symbols indicate measured steady-state concentrations of O_2 (○) and H_2S (●). Boxes indicate modeled sulfate reduction rates.

DISCUSSION

Microzonation of O_2 respiration, H_2S oxidation, and SO_4^{2-} reduction. The high spatial resolution of the microelectrode methods described above made it possible to determine the depth distribution of respiratory processes involved in the sulfur cycle of an aerobic biofilm. This is, to our knowledge, the first study of sulfate reduction and its interaction with other respiratory processes in aerobic biofilms. The sulfur cycle in the biofilm showed a close coupling between SO_4^{2-} reduction and reoxidation of H_2S with oxygen or nitrate.

(i) Sulfate reduction. When the biofilm was incubated in a mixture of SO_4^{2-}, NO_3^-, and NH_4^+, sulfate reduction occurred in the deeper, anoxic part of the biofilm and was spatially separated from H_2S oxidation, which took place at the bottom of the O_2 respiration zone (Fig. 2). The presence of 0.5 mM NO_3^- in the medium gave rise to a denitrifying zone between the aerobic part of the biofilm and the SO_4^{2-} reduction zone. Denitrification in trickling-filter biofilms has recently been investigated with microsensors (17, 71). These studies demonstrated the presence of a 0.5- to 0.8-mm-thick denitrifying zone below the aerobic zone in a biofilm incubated with 0.5 mM NO_3^-. Denitrification probably inhibited sulfate reduction, as indicated by the linear H_2S profile above the sulfate reduction zone (Fig. 2A).

(ii) Anaerobic H_2S oxidation. Despite the presence of nitrate, no anaerobic H_2S oxidation with NO_3^- was found in that experiment. Thus denitrification was not coupled to sulfide oxidation. This was surprising because several unicellular sulfur bacteria are capable of anaerobic H_2S oxidation with NO_3^- (9, 48, 49, 52, 81). A *Thiobacillus denitrificans* strain capable of H_2S oxidation with NO_3^- and N_2O was recently isolated from trickling-filter biofilms (16). In our experiment, incubation of the biofilms in tap water without NO_3^- or NH_4^+ for 1 to 3 days could have favored other biofilm processes, outcompeted anaerobic H_2S-oxidizing bacteria, or inhibited synthesis of important enzymes for the reaction.

In another experiment anaerobic H_2S oxidation could, however, be induced by addition of NO_3^- to the biofilm medium (Fig. 5C and D). The relatively long induction period observed in that experiment (16 h) would be expected if inducible enzyme systems for anaerobic H_2S oxidation had to be synthesized by denitrifying bacteria. Sørensen (78) found that denitrification could be induced by NO_3^- in reduced sediments after a lag period of 15 to 20 h. The denitrification capacity of *T. denitrificans* was shown to be inhibited by O_2, and NO_3^- reductase activity was significant only with NO_3^- present under anaerobic conditions (36, 49). When a freshly collected biofilm was incubated with NO_3^- and NH_4^+, no lag period was observed and a clear separation of O_2 and H_2S profiles indicated that anaerobic H_2S oxidation had taken place (53).

(iii) Aerobic H_2S oxidation and O_2 respiration. Despite an O_2 penetration of only 0.2 to 0.4 mm, it was possible to describe subzones with high or low O_2 respiration activities within the aerobic zone (Fig. 2B). The highest O_2 respiration rate was found in the uppermost 0.0 to 0.1 mm, where large amounts of organic substrate from the overlying water were available. Another zone of high O_2 respiration activity was found at the O_2/H_2S interface (Fig. 2B).

A similar distribution of O_2 respiration activity has been demonstrated in laboratory (66) and in situ (26) studies of oxygen consumption in coastal marine sediments. H_2S became oxidized with O_2 in a 0.1- to 0.3-mm thin zone (Fig. 2B

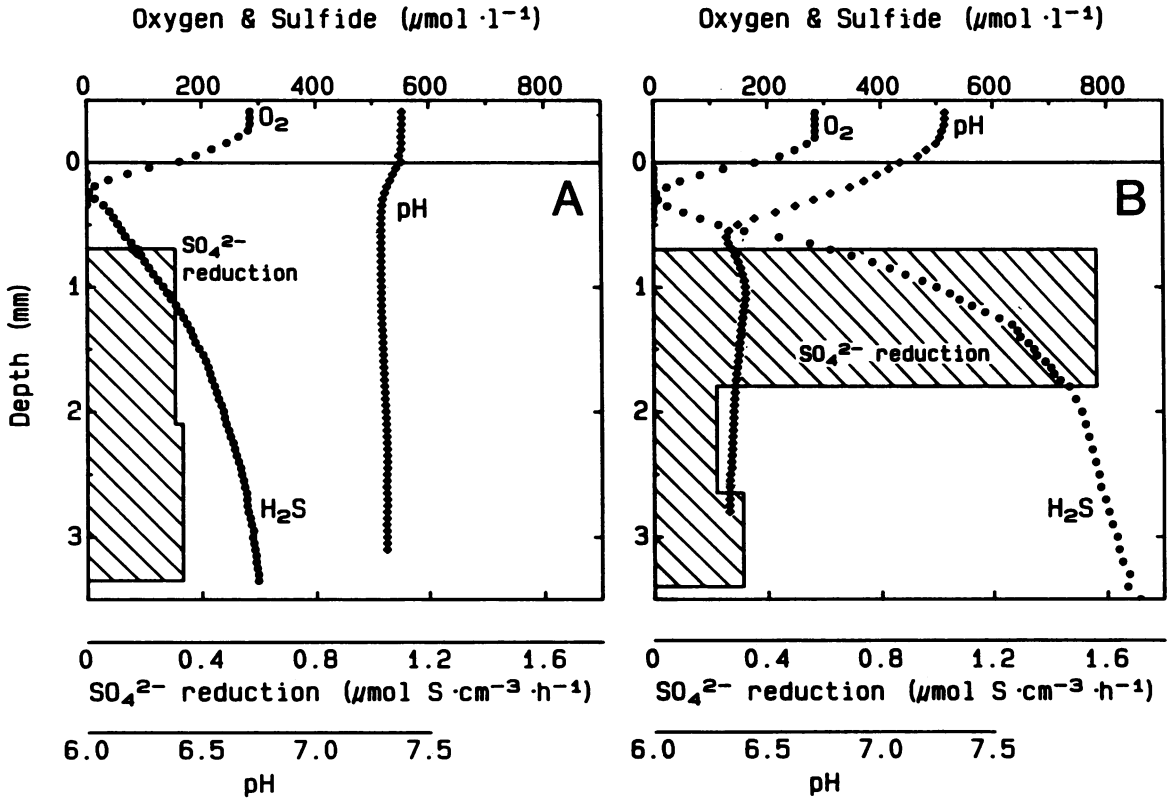

FIG. 4. Sulfate reduction as a function of organic substrate in the overlying water. The 3.5-mm-thick biofilm was incubated in 50 mM Tris-buffered medium (pH 7.35) containing 0.8 mM SO_4^{2-}. (A) Control without added organic substrate. (B) With 5 mM glucose added. Symbols indicate measured steady-state O_2 concentrations (○), pH (◆), and H_2S concentration (●). Boxes indicate modeled specific reaction rates.

and 5B). Such an extremely narrow reaction zone of O_2 and H_2S is normally found associated with bacterial H_2S oxidation, as has been demonstrated in both natural communities (41, 45) and gradient-pure cultures of sulfide-oxidizing bacteria (60, 61).

High reaction rates and a narrow reaction zone of O_2 and H_2S in the biofilms resulted in an average turnover time of only 4 to 7 s for both O_2 and H_2S in the reaction zone (Table 1). The turnover of H_2S and O_2 in the biofilm was extremely fast compared with known rates of spontaneous chemical reaction of H_2S and O_2. The half-life of H_2S during a purely chemical oxidation with O_2 in water at room temperature has been reported to be in the range of 30 min to several hours (20, 57, 58). Even when the chemical reaction is speeded up with catalysts, the half-life of H_2S is in the order of minutes (11). Aerobic H_2S oxidation in the biofilm was therefore clearly due to bacteria which were far more efficient than the chemical reaction.

Average consumption rates of O_2 and H_2S in the reaction zone could be calculated from the product of the reaction rate and the depth of the reaction zone (Table 1). The molar H_2S/O_2 consumption ratio was found to be 0.66. This ratio is close to the H_2S/O_2 consumption ratio of 0.61 predicted for complete oxidation of H_2S to SO_4^{2-} with concurrent CO_2 fixation as described in a pure-culture study of the filamentous sulfur bacterium *Beggiatoa* sp. (60). Bacterial H_2S oxidation with oxygen can be catalyzed by both unicellular and filamentous colorless sulfur bacteria (50). Although filamentous sulfur bacteria of the genus *Thiothrix* are often found in sewage treatment plants (63), no filamentous sulfur bacteria were observed in the trickling-filter biofilms we investigated. Biofilms kept in stagnant water for prolonged periods became anoxic, and the biofilm surface appeared white as a result of precipitation of elemental sulfur. Microscopy of this elemental sulfur layer demonstrated the presence of many small unicellular bacteria distributed between the sulfur granules, which could be thiobacilli. A distinct layer of elemental sulfur was not observed in fresh biofilms incubated under aerobic conditions.

Diffusion coefficients. The diffusion coefficients of O_2 and H_2S in the biofilm are key parameters for the modeling of reaction rates. Unfortunately, only a few studies have attempted to measure actual values of diffusion coefficients for these solutes in undisturbed biofilms (31, 47, 60, 67, 73). Whereas experimental techniques have been developed recently to determine diffusion coefficients for gases in living biofilm samples (23, 67), similar techniques have not been used for ionic species. Diffusion of ions is affected by interactions with other charged species in the biofilm, giving rise to phenomena such as counterdiffusion and codiffusion, which conserve the charge equilibrium between the biofilm and the overlying water (3, 54). It is therefore of importance to measure diffusion coefficients in undisturbed, biologically active biofilm samples, because inactivation with, for example, heavy-metal ions may change the electrical and chemical properties dramatically (67).

We have used a value of $(1.44 \pm 0.08) \times 10^{-5}$ cm^2 s^{-1} (20°C) for the apparent O_2 diffusion coefficient in the biofilm.

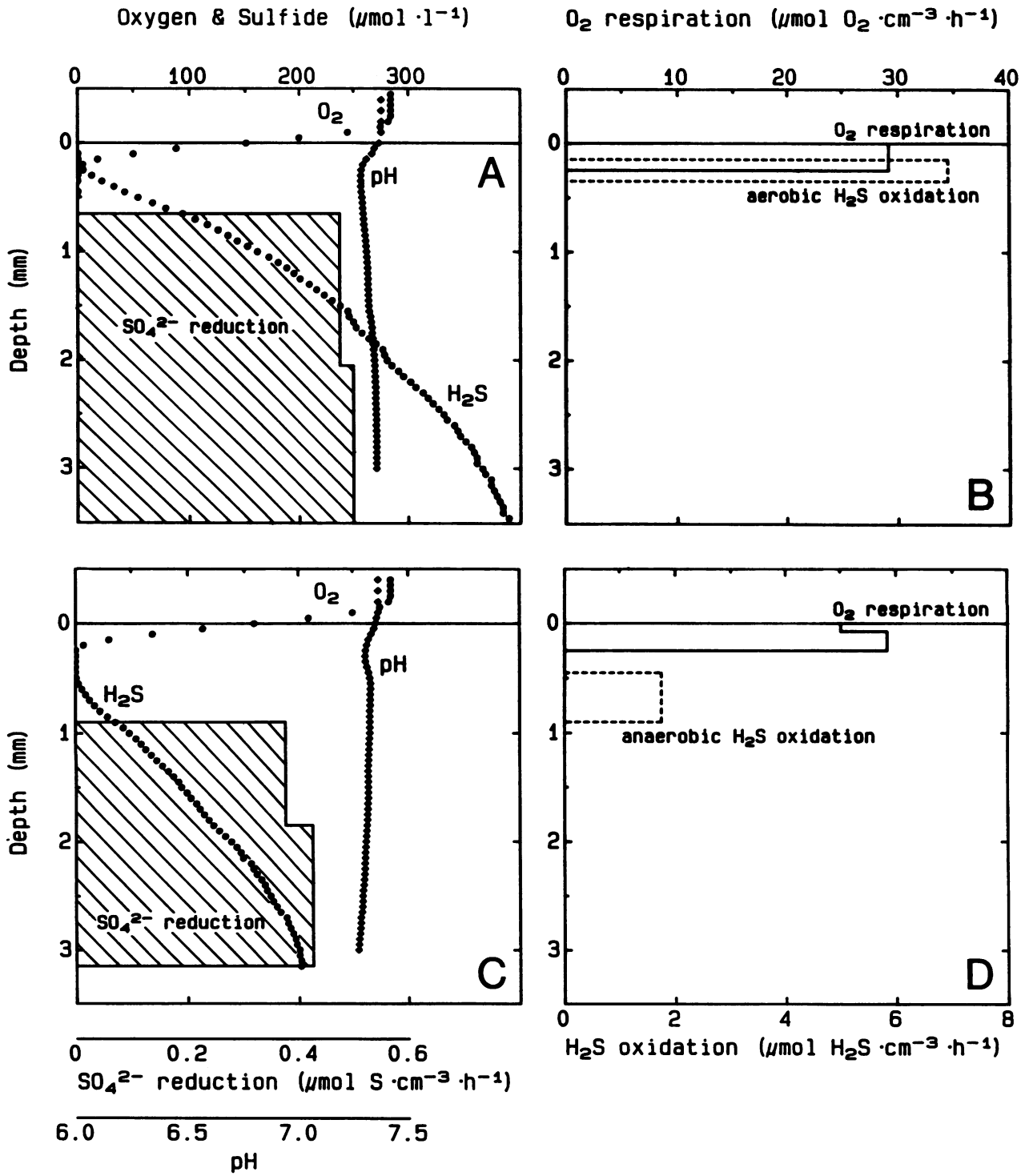

FIG. 5. Effect of nitrate on the microzonation of O_2 respiration, SO_4^{2-} reduction, and H_2S oxidation. The 3.5-mm-thick biofilm ws incubated in 50 mM Tris-buffered medium (pH 7.35) containing 0.8 mM SO_4^{2-}. (A and B) Control without nitrate in the medium. (C and D) with 500 µM nitrate added to the medium and incubated for 16 h. Symbols indicate measured steady-state O_2 concentration (○), pH (◆), and H_2S concentration (●). Boxes indicate modeled specific reaction rates.

This value was determined by the microelectrode technique of Revsbech (67) in an inactivated biofilm with an O_2 microelectrode and also with a combined O_2/N_2O microelectrode in an undisturbed biofilm of the same type as we investigated (23). The diffusion coefficient of total sulfide is more problematic because it is determined by the pH-dependent equilibria between ionic species (HS^-, S^{2-}) and gaseous species (H_2S) of sulfide. H_2S is the dominant species

at pH < 7, whereas HS^- is dominant at pH > 7 and is subject to electric interactions with other ions.

We have used a value of $(1.39 \pm 0.05) \times 10^{-5}$ cm^{-2} s^{-1} determined by Nelson et al. (60) at 20°C and pH 8.4 in sterile anaerobic agar medium with a porosity close to 1. This value is close to the value of 1.52×10^{-5} cm^{-2} s^{-1} calculated for 20°C from radiotracer measurements in cyanobacterial mats (47, 73). It is probably somewhat overestimated, since microbial metabolism of sulfide was not totally inhibited during the experiment. Although the assumed value for the H_2S diffusion coefficient used in this study may differ from the actual value by a few percent, it will, however, be of minor importance; an uncertainty of 10% in the value of the diffusion coefficient would result in an uncertainty of 10% in all calculated fluxes and reaction rates. As mentioned above, calculations of the molar H_2S/O_2 consumption ratio in the H_2S-oxidizing zone gave values close to the expected stoichiometric ratio, thus indicating that the diffusion coefficient used for H_2S was a reasonable estimate.

Effects of sulfate and organic matter. (i) Sulfate. When the biofilm was incubated with 0.5 mM SO_4^{2-} the sulfate reduction activity was found to be constant with depth throughout the sulfate reduction zone (Fig. 2A), indicating that the kinetics of SO_4^{2-} reduction were zero order with respect to SO_4^{2-}. It is reasonable to assume that SO_4^{2-} was absent below the sulfate reduction zone because an elevation of the SO_4^{2-} concentration in the water phase extended the sulfate reduction zone deeper into the biofilm (Fig. 3).

The kinetics of sulfate reduction have been studied in biofilm reactors (64) and in pure cultures of SO_4^{2-}-reducing bacteria (35). Both studies demonstrated saturation kinetics of SO_4^{2-} reduction with half-saturation constants (K_m) ranging from 1.44 μM SO_4^{2-} in anaerobic biofilms to 5 to 10 μM in freshwater *Desulfovibrio* strains. Above these concentrations, SO_4^{2-} reduction kinetics were zero order. Zero-order kinetics imply that increasing SO_4^{2-} concentrations in the overlying water should not increase the specific activity in the active layers but should affect only the extension of the sulfate reduction zone. When SO_4^{2-} concentrations in the overlying water were increased from 0.5 to 1 and 1.5 mM, we observed an extension of the SO_4^{2-} reduction zone from 1 mm (Fig. 2A) to 1.5 mm (Fig. 3A) and 2.5 mm (Fig. 3B). There was, however, a decrease in sulfate reduction activity in the active layers when the SO_4^{2-} concentration was increased. A possible explanation could be a lower availability of organic electron donors diffusing into the sulfate reduction zone from below, when SO_4^{2-} became available for sulfate-reducing bacteria in deeper layers of the biofilm. The total sulfate reduction rate increased, however, as a consequence of the deeper sulfate reduction zone.

(ii) Organic matter. Sulfate reduction activity is determined by the availability of both the electron acceptor (SO_4^{2-}) and organic electron donors. A nearly constant distribution of sulfate reduction activity over the active layer was found in all experiments with low levels of organic matter in the medium. This indicated that sulfate-reducing bacteria were uniformly distributed and that they received organic electron donors primarily from endogenous sources within the biofilm. When glucose was added to a final concentration of 5 mM in the medium, a large increase in the sulfate reduction activity was observed in the upper part of the sulfate reduction zone (Fig. 4). The total rate of sulfate reduction increased as a result of addition of organic matter by a factor of 2 relative to the control, from 0.084 to 0.21 μmol of SO_4^{2-} cm^{-2} h^{-1}. Although glucose is not known to be a major substrate for sulfate-reducing bacteria (65, 84), it can be metabolized by most fermentative bacteria. Addition of glucose therefore stimulated overall heterotrophic activity in the upper part of the biofilm and also increased the availability of fermentation products which could be metabolized by sulfate-reducing bacteria. Sulfate reduction activity was therefore stimulated in the upper part of the biofilm by organic electron donors diffusing downward from the oxic layers where glucose was metabolized.

An increased metabolic activity of the biofilm was also demonstrated by an increase in oxygen consumption from 0.42 to 0.53 μmol cm^{-2} h^{-1} and a sharp decrease in pH from 7.3 to 6.3 through the oxic zone of the biofilm (Fig. 4B). In the deeper part of the biofilm, sulfate reduction activity was almost unaffected by external addition of organic matter to the medium, indicating that the added electron donors did not reach these layers.

Quantitative aspects. (i) O_2 respiration rates. We found very high specific and total O_2 respiration rates in the biofilms. Specific respiration rates ranged from 15 to 30 μmol of O_2 cm^{-3} h^{-1} over a zone of 0.0 to 0.2–0.4 mm. Total rates thus ranged from 0.4 to 0.7 μmol of O_2 cm^{-2} h^{-1}. The observed O_2 penetration depths and specific rates are in good agreement with specific rates of O_2 respiration found in earlier studies of trickling-filter biofilms (68), microbial mats (44), and natural biofilms from eutrophic streams (62).

Specific O_2 respiration rates in the biofilms were found to be a factor of ca. 100 higher than rates in coastal marine sediments. The O_2 respiration zone in biofilms was, however, compressed about 10-fold relative to sediments, and the total respiration rate was therefore only ca. 10-fold higher (26, 66).

The specific O_2 respiration is zero order with respect to O_2 because of the low K_m values of ca. 1 μM (30), whereas the total O_2 respiration depends on the oxygen penetration depth. For zero-order kinetics and a constant reaction rate with depth, it has been shown that the depth of O_2 penetration, z_{max}, is determined by both specific activity and the rate of diffusive supply of O_2 to the biofilm (66):

$$z_{max} = (2C_0D_s/R)^{1/2} \quad (5)$$

where C_0 is the oxygen concentration at the biofilm surface, D_s is the apparent diffusion coefficient, and R is the depth-independent rate of O_2 respiration. By use of equation 5 the O_2 penetration in the presence of a diffusive boundary layer was calculated from average R values and from C_0 values measured in our experiments. The calculated z_{max} values were in all cases similar to the observed O_2 penetration depths. Oxygen transport from the mixed water to the biofilm occurs through the diffusive boundary layer, which imposes a mass transfer resistance on the supply of oxygen (5). The importance of this mass transfer resistance for the total O_2 consumption was demonstrated by the finding of much higher z_{max} values when we repeated the calculations, without taking the boundary layer into account, by using the O_2 concentration in the mixed water phase as C_0. Oxygen penetration depths were therefore reduced by 20 to 40% in the presence of a diffusive boundary layer, and total O_2 consumption by the biofilm was strongly regulated by the diffusive O_2 transport between the water and the biofilm. This result is in good agreement with results of earlier studies of O_2 consumption in biofilms (51). The rate of diffusive O_2 supply is regulated by the thickness of the diffusive boundary layer, which varies with respect to both the flow velocity of the overlying water and the surface topography of the biofilm (25, 44, 46). Comparisons of total

TABLE 2. Molar ratio of O_2 respiration to SO_4^{2-} reduction in a biofilm[a]

Substrate	Reaction zone[b] (mm)	Reaction rate (μmol/cm^3/h)	Total rate[c] (μmol/cm^2/h)	Flux[d] (μmol/cm^2/h)
O_2	0–0.1	17.45	0.390[e]	0.386[e]
	0.1–0.275	6.79		
	0.275–0.375	9.70		
H_2S	0.2–0.475	3.47	0.095	0.092
SO_4^{2-}	1.05–2.15	0.84	0.092	0.092

[a] Calculations were done on the data shown in Fig. 2.
[b] Presented as depth intervals in the biofilms.
[c] Calculated by integrating the specific reaction rate with depth.
[d] Calculated by using Fick's first law with the linear part of the H_2S profile between the H_2S oxidation and the SO_4^{2-} reduction zone and with the linear O_2 profile in the diffusive boundary layer above the biofilm. The molar O_2/H_2S flux ratio was 4.2:1.
[e] These values refer to the entire range of O_2 depth.

oxygen consumption rates measured in different experiments are therefore difficult to interpret unless the hydrodynamic conditions are characterized.

(ii) SO_4^{2-} reduction rates. Specific sulfate reduction rates ranged from 0.2 to 1.6 μmol of S cm^{-3} h^{-1}, whereas total rates ranged from 0.1 to 0.2 μmol cm^{-2} h^{-1}. The specific rates are similar to the highest reported values for sulfate reduction in marine salt marshes and microbial mats, whereas they are 10- to 100-fold higher than the rates found in most coastal marine sediments (77). The highest specific sulfate reduction rates have been found in anaerobic bioreactor systems optimized for sulfate reduction (32, 33, 64), in which rates were 100- to 1,000-fold higher than in coastal sediments.

(iii) Importance of sulfate reduction. Sulfide was oxidized completely in the biofilm and did not escape to the overlying water in our experiments. Mass balance studies of H_2S flux in the medium would therefore not have detected sulfate reduction in the biofilms. Our results do, however, indicate that sulfate reduction is an important mineralization process in this type of biofilm (Table 2; Fig. 2). The molar ratio of O_2 respiration to sulfate reduction was close to 4:1. The use of 1 mol of oxygen or sulfate for oxidation of organic electron donors requires 4 and 8 mol of electrons, respectively. The reduction capacity of 1 mol of SO_4^{2-} is therefore equivalent to 2 mol of O_2 in terms of electron flow.

The total O_2 respiration can be used as a measure of total carbon mineralization because all H_2S produced by sulfate reduction became reoxidized, with O_2 acting as the terminal electron acceptor (Fig. 2). Oxidation of 1 mol of H_2S to SO_4^{2-} requires 2 mol of O_2 according to the equation $H_2S + 2O_2 \rightarrow SO_4^{2-} + 2H^+$. Therefore $2 \times 0.092 = 0.184$ μmol of O_2 cm^{-2} h^{-1}, or 48% of the total O_2 consumption, was used for H_2S oxidation in the biofilm (Table 2) while the remaining 52% was used mostly for heterotrophic respiration and nitrification. Sulfate reduction could therefore account for almost 50% of the total oxidation of organic carbon in the biofilm investigated. Similar calculations for our other experimental data showed that SO_4^{2-} reduction accounted for 40 to 50% of total carbon mineralization, with molar ratios of O_2 respiration to SO_4^{2-} reduction ranging from 4:1 to 5:1.

When anaerobic H_2S oxidation with NO_3^- took place (Fig. 5C), O_2 uptake and SO_4^{2-} reduction were uncoupled, since H_2S became oxidized with NO_3^- in the anaerobic part of the biofilm. The molar ratio of O_2 respiration to SO_4^{2-} reduction was 8:1. Of the total mineralization of organic matter by O_2 and SO_4^{2-}, the SO_4^{2-} reduction could maximally account for 20%. This percentage is, however, an overestimate because denitrification activity coupled to oxidation of H_2S and organic matter was not included in the calculated rate of total organic carbon mineralization.

Whereas it is well known that SO_4^{2-} reduction is an important process in marine ecosystems (34, 37, 40), the demonstrated importance of sulfate reduction in the metabolism of aerobic trickling-filter biofilms is new and may have important implications for future designs of trickling filters optimized for organic carbon removal. Sulfate reduction is known to catalyze the degradation of certain xenobiotic compounds (6), and trickling-filter biofilms with a significant sulfate reduction activity may therefore have a high potential for transformation of such xenobiotics.

Sulfate reduction is probably also an important process in other types of biofilms. Aerobic biofilms growing on concrete sewers or on metal surfaces may cause severe corrosion as a result of the presence of electrochemical concentration cells and acid generation when sulfide is oxidized. Sulfate-reducing bacteria are closely associated with these processes, although the mechanisms are still unclear (1, 27, 65, 76). Our understanding of the interactions between respiratory processes and corrosion induced by biofilms may be improved by the use of microsensor techniques. Another field in which sulfide, pH and oxygen microgradients are of major interest is that of microbial mats and sediments, where high sulfate reduction activity occurs close to the sediment surface (2, 10, 43, 77) and anaerobic microniches may occur in the oxic layers (38). Rates of sulfate reduction and sulfide oxidation calculated from measurements with sulfide microelectrodes in these systems may, however, underestimate the real reaction rates if large amounts of iron and manganese are present which can react with H_2S and form insoluble metal sulfides, elemental sulfur, and polysulfides (70, 82). In our biofilms the amounts of metal were probably small, because black iron sulfide and other metal sulfides were not observed. Microsensors are ideal tools for studying respiratory processes in compact microbial communities. The high spatial resolution of the microsensors enabled us for the first time to study the sulfur cycle in aerobic biofilms and to measure reaction rates of sulfate reduction and H_2S oxidation. We were able to demonstrate the zonation of respiratory processes in the biofilm with O_2 respiration occurring in the upper 0.2 to 0.4 mm, denitrification occurring just below the aerobic zone, and sulfate reduction occurring in the deeper, anoxic layers. Preliminary investigations also indicated the presence of methanogenesis, because CH_4 was detected in samples from the deepest parts of the biofilm. The same vertical zonation of respiratory processes found on a centimeter or meter scale in aquatic sediments is therefore present within a few millimeters in biofilms.

ACKNOWLEDGMENTS

We thank Annie Glud, Lars B. Pedersen, and Elsebeth Thomsen for construction of O_2 microelectrodes and Niels Peter Revsbech for many helpful discussions and for construction of pH microelectrodes.

Financial support was provided by the Danish Center for Environmental Biotechnology, the Nordic Program Committee on Biotechnology, and the Max Planck Society (Germany).

REFERENCES

1. **Bak, F., H. G. Behrendt, and W. Kleinitz.** 1990. Bakterielle Korrosion in einer Reinölleitung. Erdöl Erdgas Kohle **106:**109–113.

2. **Bauld, J., L. A. Chambers, and G. W. Skyring.** 1979. Primary productivity, sulfate reduction and sulfur isotope fractionation in algal mats and sediments of Hamelin Pool, Shark Bay, W.A. Aust. J. Mar. Freshwater Res. **30:**753–764.
3. **Ben-Yaakov, S.** 1972. Diffusion of sea water ions. I. Diffusion of sea water into a dilute solution. Geochim. Cosmochim. Acta **36:**1395–1406.
4. **Berner, R. A.** 1980. Early diagenesis: a theoretical approach. Princeton University Press, Princeton, N.J.
5. **Boudreau, B. P., and N. L. Guinasso.** 1982. The influence of a diffusive sublayer on accretion, dissolution, and diagenesis at the sea floor, p. 115–145. *In* K. A. Fanning and F. T. Manheim (ed.), The dynamic environment of the ocean floor. Lexington Books, Lexington, Mass.
6. **Bouwer, E. J.** 1989. Transformation of xenobiotics in biofilms, p. 251–269. *In* W. G. Characklis and P. A. Wilderer (ed.), Structure and function of biofilms. John Wiley & Sons, Inc., New York.
7. **Broecker, W. S., and T. H. Peng.** 1974. Gas exchange rates between air and sea. Tellus **26:**21–35.
8. **Bungay, H. R., W. J. Whalen, and W. M. Sanders.** 1969. Microprobe techniques for determining diffusivities and respiration rates in microbial slimes. Biotechnol. Bioeng. **11:**765–772.
9. **Cadenhead, P., and K. L. Sublette.** 1990. Oxidation of hydrogen sulfide by thiobacilli. Biotechnol. Bioeng. **35:**1150–1154.
10. **Canfield, D. E., and D. J. Des Marais.** 1991. Aerobic sulfate reduction in microbial mats. Science **251:**1471–1473.
11. **Chen, K. Y., and J. C. Morris.** 1972. Oxidation of sulfide by O_2—catalysis and inhibition. J. Sanit. Eng. **98:**215–227.
12. **Chen, Y. S., and H. R. Bungay.** 1989. Microelectrode studies of oxygen transfer in trickling filter slimes. Biotechnol. Bioeng. **23:**781–792.
13. **Christensen, P. B., L. P. Nielsen, N. P. Revsbech, and J. Sørensen.** 1989. Microzonation of denitrification activity in stream sediments as studied with a combined oxygen and nitrous oxide microsensor. Appl. Environ. Microbiol. **55:**1234–1241.
14. **Cline, J. D.** 1969. Spectrophotometric determination of hydrogen sulfide in natural waters. Limnol. Oceanogr. **14:**454–458.
15. **Cohen, Y.** 1984. Oxygenic photosynthesis, anoxygenic photosynthesis, and sulfate reduction in cyanobacterial mats, p. 435–441. *In* M. J. Klug and C. A. Reddy (ed.), Current perspectives in microbial ecology. American Society for Microbiology, Washington, D.C.
16. **Dalsgaard, T., and F. Bak.** Submitted for publication.
17. **Dalsgaard, T., and N. P. Revsbech.** Submitted for publication.
18. **DeBeer, D.** 1990. Microelectrode studies in biofilms and sediments. Ph.D. thesis. University of Amsterdam, Amsterdam, The Netherlands.
19. **DeBeer, D., and J. P. R. A. Sweerts.** 1989. Measurement of nitrate gradients with an ion selective microelectrode. Anal. Chim. Acta **219:**351–356.
20. **Eary, L. E., and J. A. Schramke.** 1990. Rates of inorganic oxidation reactions involving dissolved oxygen, p. 379–396. *In* D. C. Melchior and R. L. Basset (ed.), Chemical modelling of aqueous systems II. American Chemical Society, Washington, D.C.
21. **Frevert, T., and H. Galster.** 1978. Schnelle und einfache Methode zur In-Situ-Bestimmung von Schwefelwasserstof in Gewässern und Sedimenten. Schweiz. Z. Hydrol. **40:**199–208.
22. **Giggenbach, W.** 1971. Optical spectra of highly alkaline sulfide solutions and the second dissociation constant of hydrogen sulfide. Inorg. Chem. **10:**1333–1338.
23. **Glud, R. N., and K. Jensen.** Unpublished results.
24. **Glud, R. N., N. B. Ramsing, and N. P. Revsbech.** Photosynthesis and photosynthesis-coupled respiration in natural biofilms quantified with oxygen microsensors. J. Phycol., in press.
25. **Gundersen, J. K., and B. B. Jørgensen.** 1990. Microstructure of diffusive boundary layers and the oxygen uptake of the sea floor. Nature (London) **345:**604–607.
26. **Gundersen, J. K., and B. B. Jørgensen.** 1991. Fine scale in situ measurements of oxygen distribution in marine sediments. Kiel. Meeresforsch. Sonderh. **8:**376–380.
27. **Hamilton, W. A.** 1985. Sulfate-reducing bacteria and anaerobic corrosion. Annu. Rev. Microbiol. **39:**195–217.
28. **Hamilton, W. A.** 1987. Biofilms: microbial interactions and metabolic activities, p. 361–385. *In* M. Fletcher, T. R. G. Gray, and J. G. Jones (ed.), Ecology of microbial communities. Cambridge University Press, Cambridge.
29. **Hamilton, W. A., and W. G. Characklis.** 1989. Relative activities of cells in suspension and in biofilms, p. 199–219. *In* W. G. Characklis and P. A. Wilderer (ed.), Structure and function of biofilms. John Wiley & Sons, Inc., New York.
30. **Hao, O. J., M. G. Richard, and D. Jenkins.** 1983. The half saturation coefficient for dissolved oxygen: a dynamic method for its determination and its effect on dual species competition. Biotech. Bioeng. **25:**403–416.
31. **Hofman, P. A. G., S. A. de Jong, E. J. Wagenvoort, A. J. J. Sandee.** 1991. Apparent sediment diffusion coefficients for oxygen and oxygen consumption rates measured with microelectrodes and bell jars: application to oxygen budgets in estuarine intertidal sediments (Osterschelde, SW Netherlands). Mar. Ecol. Prog. Ser. **69:**261–272.
32. **Holder, G. A., R. Van Oorschot, and J. Hauser.** 1989. Experimental and theoretical studies of sulfide generation in sewerage systems. Water Sci. Technol. **21:**757–768.
33. **Holder, G. A., G. Vaughan, and W. Drew.** 1985. Kinetic studies of the microbiological conversion of sulphate to hydrogen sulphide and their relevance to sulphide generation within sewers. Water Sci. Technol. **17:**183–196.
34. **Howarth, R. W.** 1984. The ecological significance of sulfur in the energy dynamics of salt marsh and coastal marine sediments. Biogeochemistry **1:**5–27.
35. **Ingvorsen, K., and B. B. Jørgensen.** 1984. Kinetics of sulfate uptake by freshwater and marine species of *Desulfovibrio*. Arch. Microbiol. **139:**61–66.
36. **Justin, P., and D. P. Kelly.** 1978. Metabolic changes in *Thiobacillus denitrificans* accompanying the transition from aerobic to anaerobic growth in continuous chemostat culture. J. Gen. Microbiol. **107:**131–137.
37. **Jørgensen, B. B.** 1977. The sulfur cycle of a coastal marine sediment (Limfjorden, Denmark). Limnol. Oceanogr. **22:**814–832.
38. **Jørgensen, B. B.** 1977. Bacterial sulfate reduction within reduced microniches of oxidized marine sediments. Mar. Biol. **41:**7–17.
39. **Jørgensen, B. B.** 1978. A comparison of methods for the quantification of bacterial sulfate reduction in coastal marine sediments. I. Measurement with radiotracer techniques. Geomicrobiol. J. **1:**11–27.
40. **Jørgensen, B. B.** 1982. Mineralization of organic matter in the sea bed—the role of sulphate reduction. Nature (London) **296:**643–645.
41. **Jørgensen, B. B.** 1982. Ecology of the bacteria of the sulphur cycle with special reference to anoxic-oxic interface environments. Philos. Trans. R. Soc. London Ser. B **298:**543–561.
42. **Jørgensen, B. B.** 1987. Ecology of the sulfur cycle: oxidative pathways in sediments, p. 31–63. *In* J. A. Cole and S. Ferguson (ed.), The nitrogen and sulphur cycles. Cambridge University Press, Cambridge.
43. **Jørgensen, B. B., and Y. Cohen.** 1977. Solar Lake (Sinai). 5. The sulfur cycle of the benthic cyanobacterial mats. Limnol. Oceanogr. **22:**657–666.
44. **Jørgensen, B. B., and D. J. Des Marais.** 1990. The diffusive boundary layer of sediments: oxygen microgradients over a microbial mat. Limnol. Oceanogr. **35:**1343–1355.
45. **Jørgensen, B. B., and N. P. Revsbech.** 1983. Colorless sulfur bacteria, *Beggiatoa* spp. and *Thiovulum* spp., in O_2 and H_2S microgradients. Appl. Environ. Microbiol. **45:**1261–1270.
46. **Jørgensen, B. B., and N. P. Revsbech.** 1985. Diffusive boundary layers and the oxygen uptake of sediments and detritus. Limnol. Oceanogr. **30:**111–122.
47. **Jørgensen, B. B., N. P. Revsbech, T. H. Blackburn, and Y. Cohen.** 1979. Diurnal cycle of oxygen and sulfide microgradients and microbial photosynthesis in a cyanobacterial mat sediment.

Appl. Environ. Microbiol. **38:**46–58.
48. **Kelly, D. P.** 1989. Physiology and biochemistry of unicellular sulfur bacteria, p. 193–217. *In* H. G. Schlegel and B. Bowien (ed.), Autotrophic bacteria. Springer-Verlag, New York.
49. **Kuenen, J. G., and R. F. Beudeker.** 1982. Microbiology of thiobacilli and other sulphur-oxidizing autotrophs, mixotrophs and heterotrophs. Philos. Trans. R. Soc. London Ser. B **298:** 473–497.
50. **Kuenen, J. G., and P. Bos.** 1989. Habitats and ecological niches of chemolitho(auto)trophic bacteria, p. 53–80. *In* H. G. Schlegel and B. Bowien (ed.), Autotrophic bacteria. Springer-Verlag, New York.
51. **Kuenen, J. G., B. B. Jørgensen, and N. P. Revsbech.** 1986. Oxygen microprofiles of trickling filter biofilms. Water Res. **20:**1589–1598.
52. **Kuenen, J. G., L. A. Robertson, and H. Van Gemerden.** 1985. Microbial interactions among aerobic and anaerobic sulfur-oxidizing bacteria. Adv. Microb. Ecol. **8:**1–59.
53. **Kühl, M., and T. Dalsgaard.** Unpublished results.
54. **Li, Y., and S. Gregory.** 1974. Diffusion of ions in sea water and in deep-sea sediments. Geochim. Cosmochim. Acta **38:**703–714.
55. **Maxwell, S., and W. A. Hamilton.** 1986. Modified radiorespirometric assay for determining the sulfate reduction activity of biofilms on metal surfaces. J. Microbiol. Methods **5:**83–91.
56. **Meyer, B., K. Ward, K. Koshlap, and L. Peter.** 1983. Second dissociation constant of hydrogen sulfide. Inorg. Chem. **22:** 2345–2346.
57. **Millero, F. J.** 1986. The thermodynamics and kinetics of the hydrogen sulfide system in natural waters. Mar. Chem. **18:**121–147.
58. **Millero, F. J., and J. P. Hershey.** 1989. Thermodynamics and kinetics of hydrogen sulfide in natural waters, p. 282–313. *In* E. S. Saltzman and W. J. Cooper (ed.), Biogenic sulfur in the environment. American Society for Microbiology, Washington, D.C.
59. **Millero, F. J., T. Plese, and M. Fernandez.** 1988. The dissociation of hydrogen sulfide in seawater. Limnol. Oceanogr. **33:**269–274.
60. **Nelson, D. C., B. B. Jørgensen, and N. P. Revsbech.** 1986. Growth pattern and yield of a chemoautotrophic *Beggiatoa* sp. in oxygen-sulfide microgradients. Appl. Environ. Microbiol. **52:**225–233.
61. **Nelson, D. C., N. P. Revsbech, and B. B. Jørgensen.** 1986. Microoxic-anoxic niche of *Beggiatoa* spp.: microelectrode survey of marine and freshwater strains. Appl. Environ. Microbiol. **52:**161–168.
62. **Nielsen, L. P., P. B. Christensen, N. P. Revsbech, and J. Sørensen.** 1990. Denitrification and oxygen respiration in biofilms studied with a microsensor for nitrous oxide and oxygen. Microb. Ecol. **19:**63–72.
63. **Nielsen, P. H.** 1985. Oxidation of sulfide and thiosulfate and storage of sulfur granules in *Thiothrix* from activated sludge. Water Sci. Technol. **17:**167–181.
64. **Nielsen, P. H.** 1987. Biofilm dynamics and kinetics during high-rate sulfate reduction under anaerobic conditions. Appl. Environ. Microbiol. **53:**27–32.
65. **Postgate, J. R.** 1984. The sulphate-reducing bacteria. Cambridge University Press, Cambridge.
66. **Rasmussen, H., and B. B. Jørgensen.** Submitted for publication.
67. **Revsbech, N. P.** 1989. Diffusion characteristics of microbial communities determined by use of oxygen microsensors. J. Microbiol. Methods **9:**111–122.
68. **Revsbech, N. P.** 1989. Microsensors: spatial gradients in biofilms, p. 129–144. *In* W. G. Characklis and P. A. Wilderer (ed.), Structure and function of biofilms. John Wiley & Sons, Inc., New York.
69. **Revsbech, N. P.** 1989. An oxygen microelectrode with a guard cathode. Limnol. Oceanogr. **34:**474–478.
70. **Revsbech, N. P., P. B. Christensen, and L. P. Nielsen.** 1989. Microelectrode analysis of photosynthetic and respiratory processes in microbial mats, p. 153–163. *In* Y. Cohen and E. Rosenberg (ed.), Microbial mats: physiological ecology of benthic microbial communities. American Society for Microbiology, Washington, D.C.
71. **Revsbech, N. P., P. B. Christensen, L. P. Nielsen, and J. Sørensen.** 1989. Denitrification in a trickling filter biofilm studied by a microsensor for oxygen and nitrous oxide. Water Res. **23:**867–871.
72. **Revsbech, N. P., and B. B. Jørgensen.** 1986. Microelectrodes: their use in microbial ecology. Adv. Microb. Ecol. **9:**293–352.
73. **Revsbech, N. P., B. B. Jørgensen, T. H. Blackburn, and Y. Cohen.** 1983. Microelectrode studies of the photosynthesis and O_2, H_2S, and pH profiles of a microbial mat. Limnol. Oceanogr. **28:**1062–1074.
74. **Revsbech, N. P., B. B. Jørgensen, and O. Brix.** 1981. Primary production of microalgae in sediments measured by oxygen microprofile, $H^{14}CO_3^-$ fixation, and oxygen exchange methods. Limnol. Oceanogr. **26:**717–730.
75. **Revsbech, N. P., L. P. Nielsen, P. B. Christensen, and J. Sørensen.** 1988. Combined oxygen and nitrous oxide microsensor for denitrification studies. Appl. Environ. Microbiol. **54:** 2245–2249.
76. **Schashl, E.** 1980. Elemental sulfur as a corrodent in deaerated neutral aqueous solutions. Mater. Perform. **19:**9–12.
77. **Skyring, G. W.** 1987. Sulfate reduction in coastal ecosystems. Geomicrobiol. J. **5:**295–374.
78. **Sørensen, J.** 1978. Capacity for denitrification and reduction of nitrate to ammonia in a coastal marine sediement. Appl. Environ. Microbiol. **35:**301–305.
79. **Sweerts, J. P. R. A.** 1990. Oxygen consumption processes, mineralization and nitrogen cycling at the sediment-water interface of north temperate lakes. Ph.D. thesis. University of Groningen, Groningen, The Netherlands.
80. **Sweerts, J. P. R. A., D. DeBeer, L. P. Nielsen, H. Verdouw, J. C. Van den Heuvel, Y. Cohen, and T. E. Cappenberg.** 1990. Denitrification of sulfur oxidizing *Beggiatoa* spp. mats on freshwater sediments. Nature (London) **344:**762–763.
81. **Timmer-Ten Hoor, A.** 1975. A new type of thiosulphate oxidizing, nitrate reducing microorganism: *Thiomicrospira denitrificans* sp. nov. Neth. J. Sea Res. **9:**344–350.
82. **van Gemerden, H., C. S. Tughan, R. de Wit, and R. A. Herbert.** 1989. Laminated microbial ecosystems on sheltered beaches in Scapa Flow, Orkney Islands. FEMS Microb. Ecol. **62:**87–102.
83. **Ward, D. M., T. A. Tayne, K. L. Anderson, and M. M. Bateson.** 1987. Community structure and interactions among community members in hot spring cyanobacterial mats, p. 179–210. *In* M. Fletcher, T. R. G. Gray, and J. G. Jones (ed.), Ecology of microbial communities. Cambridge University Press, Cambridge.
84. **Widdel, F.** 1988. Microbiology and ecology of sulfate- and sulfur-reducing bacteria, p. 469–585. *In* A. J. B. Zehnder (ed.), Biology of anaerobic microorganisms. John Wiley & Sons, Inc., New York.